LHCb RICH 2 Mechanics

M. Alemi[4], S. Cuneo[2], C.J. Densham[5], V. Gracco[2], P. Musico[2], A. Petrolini[2], M. Sannino[2], F.J.P. Soler[3,5], S.A. Temple[5], O. Ullaland[1], D. Voillat[1], P. Wertelaers[1] and P. Wicht[1].

[1] European Organization for Nuclear Research, Geneva, Switzerland
[2] Universita Dipart. di Fisica, di Genova, Genova, Italy
[3] University of Glasgow, Glasgow, UK
[4] INFN, Universita di Milano, Milano, Italy
[5] Rutherford Appleton Laboratory, UK

Abstract

This note gives an overview of the status of the mechanics for the RICH 2 detector in the LHCb experiment at LHC.

1 Introduction.

The acceptance of the LHCb RICH 2 detector covers the angular range up to ±120 mrad in the horizontal projection, ZX plane, and up to ±100 mrad in the vertical projection, YZ plane. The enclosed gas volume extends from z=9450 mm to z=11470 mm. The gas is CF_4 at atmospheric pressure and ambient temperature. The optical system consists of two spherical mirror arrays and two flat mirror arrays. The radius of curvature of the spherical mirrors is 8000 mm. The tangent to the spherical mirror plane at x=0 in the ZX plane is ±450 mrad with respect to the X axis. The flat mirror plane is tilted in the ZX plane by ±140 mrad with respect to the X axis. The detector plane is thereby defined between $[x, z]$ [±4052,10342] and [±3653,10827]. The flat mirror plane is outside the 120 mrad acceptance. The mean Cherenkov radiator length is about 1670 mm. Figure 1 gives the horizontal view and the side view. Figure 2 gives the vertical projections of the detector. Reference [1] gives an overview of the evolution of the geometry of RICH 2 as of the Technical Proposal [2].

2 The main structure.

The supporting mechanical structure is an open rectangular space frame where all structural components are kept outside the acceptance of the LHCb spectrometer which is ±300 mrad in the horizontal plane (the bending plane) and ±250 mrad in the vertical plane. The main building block for this structure is a stainless steel high I-profile beam of 37.7 cm^2. Further stabilisation of the structure is obtained by interconnecting the stainless steel beams with stainless steel sheets. The structure is welded and the total weight is about 11000 kg.

3 Entrance and exit windows.

The entrance and exit windows are light weight composite material panels made from 48 mm polymethacrylimid, PMI, foam with 1 mm thick glass fibre reinforced epoxy sheets, G10, on each side. A thin skin of metal foil is added to the G10 plates which faces the Cherenkov gas volume. The total radiation length for each panel is 1.4 % X_0. Aluminium ⌊⌋-profiles are used as a frame for the panels. Classic polytetrafluoro-ethylene, PTFE (Viton), O-rings ensure the gas tightness between these frames and the supporting mechanical structure. Note that both sides are machined (Figure 4).

A tube, coaxial to the vacuum chamber, runs through the detector. The tube is 3 mm thick and made from G10. It has a 30 mm larger radius than the vacuum chamber. This distance is needed to accommodate the bake-out equipment for the vacuum chamber. The tube is fixed to the entrance and exit window and the leak tightness is again ensured by PTFE O-rings. The mechanical reinforcements needed in this area are made of polycarbonate in order to keep the radiation length as long as possible (Figure 3). The windows are designed to withstand the hydrostatic pressure of the Cherenkov gas +200 -100 Pa as defined at the top of the detector. The proposed flow rate of 10 % of the total Cherenkov gas volume per hour is largely sufficient to compensate for a sudden rise or fall in the atmospheric pressure. (See reference [3]).

4 The mirror arrays and the mirror adjustments.

The spherical mirror arrays are made from a matrix of smaller hexagonal mirror segments. Each mirror is inscribed in a circle of diameter 502 mm and made from a 6 mm thick glass substrate with a UV enhanced aluminium coating. A quartz protective coating will be added onto the reflective surfaces. (See reference [4]). Only one size of mirrors is used apart from at the vertical

edges where half mirrors are introduced. Special segments have to be foreseen near to the inner tube. The minimum gap between two mirror segments is 2 mm and the largest one 16 mm. This will introduce an inefficiency of only 2.25 %. Mirror segments of different sizes are therefore not required. The acceptance of the spherical mirror arrays extend to 125.4 mrad in the horizontal plane to reflect all the Cherenkov light created by particles inside the 120 mrad acceptance. Along the vertical axis the mirror arrays extends up to about 120 mrad (Figure 1).

A 40 mm thick aluminium honeycomb flat panel is the supporting structure for a spherical mirror array. A light weight metallic structure is prefer here in order not to have any problems as to compatibility towards the fluorocarbon gas and maintaining a high degree of mechanical stability. The average overall radiation length is 3.3 % X_0. The plate is 5940 mm high and 1435 mm wide. It is tangential to the middle of the spherical mirror array and the minimum distance to it is 30 mm. Minimum clearance to the exit window is 12 mm. 80 mm high aluminium inserts are used as reinforcements of the panel at the top and at the bottom. At the bottom, this insert is firmly clamped to a 1000 mm long try-square which acts as the optical bench (Figure 5). The panel is clamped in a similar way at the top with the difference that it is there free to move in the vertical direction. The panel has only limited adjustment possibilities.

A polycarbonate ring is glued with standard epoxy resin to the back of each of the spherical mirror segments and a corresponding flexible polycarbonate membrane is inserted into the aluminium honeycomb flat panel. A polycarbonate hollow rod connects these two elements. (See reference [5] and figure 6). The angle and the position of each of the membranes are precisely machined. The mirror can be adjusted around this angle by $\pm$ 3 mrad under the action of an elastic deformation of the flexible membrane. A long term stability measurement has been done (reference [5]). This flexible mirror mount is stable in the vertical and in the horizontal projection to within 0.03 mrad over 5000 hours after the first 100 hours relaxation period.

An identical system is used for the flat mirrors. The only difference is that a small rotational freedom is introduced around the vertical axis and that the mirror segments are here assumed to be squares of 437 $\times$ 437 mm^2 (Figure 1 and figure 2).

Polycarbonate has been chosen for its excellent mechanical stability and long, 346 mm, radiation length. It also has a low, 0.2 to 0.3 %, Total Mass Loss (TML) and a low water absorption of 0.15 % [1]. Fluorocarbons can influence the geometrical stability of composites and plastic materials. These changes are connected to the TML and the amount of plastifiers in the material [6]. We started a year ago a long term stability test of polycarbonate in fluorocarbon by immersing test samples in warm, 40 °C, vapour of C_6F_{14}.

5 The quartz plate.

A plate of fused quartz separates the Cherenkov gas volume and the volume occupied by the photon detectors. The plate is made up of six 5 mm thick elements which are 400 mm wide and 450 mm high. Standard epoxy resin can be used and the glue joint is defined to better then 50 μm. The plate is held in place by a double squeezed PTFE O-ring.

6 The overall magnetic shielding.

A heavy iron structure is used to shield the photon detectors from the stray magnetic field. See reference [7] and figure 1. A triple layer of 40 mm thick soft iron interspersed by about 115 mm surrounds the sides of the detector. In addition, two 40 mm thick soft iron walls closes the front of the detector while leaving full acceptance for the Cherenkov photons focussed onto the detector plane. Calculations and measurements shows that this structure will attenuate a

[1] MATLAB: 003 and Bayer Corp. Plastics Div. Makrolon, Polycarbonate

vertical magnetic field by a factor of 13 to 15. A component along Z will be attenuated by about the same factor. For obvious reasons it is not as satisfactory for a B component along X. The attenuation is not better then a factor of 2 to 3. B_x is small in the current calculations of the magnetic field. The total weight of this structure is about 11000 kg taking the total weight of RICH 2 to about 34 ton.

With reasonable assumptions about the stray magnetic field, this structure will assure a residual magnetic flux density below 1 mT in the region of the photon detector plane. Local reduction of the flux density will be done with a cylinder made of magnetic shielding alloy, Mumetal or Permalloy C, around each HPD. This cylinder is an integral part of the HPD assembly. See reference [8] for further details.

7 The detector plane.

The Hybrid Photon Detectors (HPDs) [8] are arranged in groups of two, fixed by means of their own pins on a common multilayer board through a ZIF socket, then making an elementary subassembly unit. Each of these units are located, by means of two dowel pins, in an aluminium supporting frame that houses 8 subassemblies (15 HPDs, 7 groups of 2 plus 1 group of 1) arranged in columns. These subassemblies are mechanically fixed by means of screws that hold the HPDs back-plate through spacers made of thermoplastic resin (Figure 7).

The frame also houses one electronics board on the back of each unit. These boards are arranged vertically, for good convection heat exchange, and can be individually pulled backward sliding on their own guides. Their electrical contact with the board on the back of the HPDs which are located on the other side of the supporting structure, is ensured by means of high-density linear connectors face-mounted on the rear of this last board.

There are in total 9 supporting frames on each panel which can be individually pulled backward without disturbing the neighbouring ones, sliding on their own guides. They are fixed by means of dowel pins and screws to a main supporting frame. This main supporting frame is made of aluminium. It incorporates the 9 supporting frames and their sliding guides. Small adjustments of the HPD plane can be made. The whole assembly is installed on high precision guide-rails that allow for the extraction of the full assembly out of the vessel structure, as well as its approaching to the fixed structure.

All HPD cable will get off the HPD through its back-plate, and will be routed by the side of the supporting frame. Local strain relief of the cables to the frame can be easily foreseen.

As the power generated by the HPDs themselves is relatively low, we do not expect any problem in draining it away with natural, or eventually forced, gas flow. We suggest to investigate further this aspect, eventually considering different gases as alternative to Nitrogen, and building up a simplified model of the assembly for these tests. The heat power loss of the electronic boards on the rear side of the detector plane will probably not require a conductive cooling system as the packaging is rather open. We only arranged the boards with their faces vertically oriented, to help the conduction, and recommended forced ventilation of the whole volume where the HPDs assembly has to be installed. Fore more details, see reference [9].

8 Mechanical structure analysis

A preliminary study of the RICH 2 mechanical structure was performed to assess the response of the structure under static and dynamic loading conditions. The complexity of the geometry of the structure is such that a Finite Element Analysis is necessary to calculate the exact mechanical behaviour. Both an initial static and modal analysis have been carried out.

The rigid mechanical space frame was modelled using BEAM189 elements in the ANSYS 5.5 Finite Element package [2]. Consistent with the design, Stainless Steel Grade 304 [3] I-beams of 37.7 cm^2 sectional area were used throughout. Structural contributions from the thin stainless steel panels and the low mass composite entrance and exit windows are ignored in the calculations. The model is constrained at the nodes consistent with the 4 support positions of the structure. Loading is applied at suitable points on the structure to represent the magnetic shielding and the mirror plane assemblies. 152 kg are assumed for each of the spherical mirror planes and 140 kg for each of the flat mirror planes. In addition a gravitational acceleration is applied to allow an appropriate static analysis to be made. The model boundary conditions and geometry are displayed in figure 8. Figure 9 shows a maximum static deflection of 1.4 mm occurring at the centre of the upper longitudinal beams.

A modal analysis was performed using the same geometry and constraints to enable the determination of the first three natural frequencies of the structure. In this calculation only the mass of the magnetic shielding together with the self mass of the structure is taken into account.

- Mode 1 occurs at 1.2 Hz and involves displacement of the upper section of the structure in the Z direction .
- Mode 2 occurs at 1.4 Hz and again involves the movement of the upper section in the Z direction, this time twisting about a central axis
- Mode 3 occurs at 2.9 Hz. In this mode the upper section is moving in the X direction.

All 3 modes are caused by beams bending in the proximity of the detector planes. Figure 10 shows the plot for mode 3 and figure 11 gives a close-up for this mode next to the detector plane.

Further work is now envisaged to subsequently optimise the mechanical design with regards to the important stability and accuracy requirements of the detector.

9 Installation procedure.

It is thought that the experimental zone will not be a good place to mount the RICH 2 and to do the alignment of the optical system, as it will be very difficult to request a near dust free environment for a longer period. We therefore propose to do it in the following steps :

1. The main structure with the Cherenkov gas enclosure is pre-mounted and leak tested at the point of fabrication. The leak testing is done at 5000 Pa overpressure with added support frames for the windows and with a replacement wall for the quartz plate. The leak rate should be ≤ 50 l/h at that pressure.
2. This structure is then transported to CERN and remounted in a surface building together with the magnetic shield which is inside the Cherenkov gas volume, the quartz plates and the mechanics for the detector planes. All instrumentation for the detector control systems are also installed at this time. See reference [10] for detailed requirements.
3. The optical benches are installed and aligned together with the support plates for the spherical mirror segments equipped with the adjustable mirror mounts.
4. The spherical mirrors are then installed and aligned. See references [10] and [4] for details.
5. Identical procedure is repeated for the flat mirrors.

[2] ANSYS 5.5 Elements Reference Manual 4-993

[3] E=200 GPa, v=0.3, Dens=7930 Kg/m^3

6. The total optical system is checked for possible time dependent deformations and re-aligned if necessary.

7. The RICH 2 detector is then transported to the experimental zone and placed on the beam line. The detector therefore has to be smaller than the 10.00 m diameter of PX shaft for equipment access.

8. The rest of the magnetic shielding is mounted as well as the detector planes.

9. The total optical system is checked for possible deformations and re-aligned if necessary. The exit window will have to be off and the pre-shower detector withdrawn for the re-alignment. As this alignment procedure is a fast operation, it should not jeopardise the integrity of the detector.

References

[1] D. Websdale, 'Proposed adjustment of the geometry of RICH 2', LHCb 99-033, RICH, INTERNAL NOTE, 7.9.1999

[2] LHCb Technical Proposal, CERN/LHCC 98-4

[3] M. Bosteels, F. Hahn, S. Haider, R. Lindner and O. Ullaland, 'LHCb RICH Gas system proposal', LHCb 2000-079 RICH.

[4] C. D'Ambrosio, L. Fernandez, M. Laub and D. Piedigrossi, 'The Optical systems of LHCb RICH: A study of the mirror walls and mirror specifications', LHCb 2000-071 RICH

[5] C. D'Ambrosio, M. Laub and P. Wertelaers, 'An experimental set-up to measure the long-term stability of large-mirror supports', LHCb 2000-020 RICH

C. D'Ambrosio, M. Laub, D. Piedigrossi, P. Wertelaers and P. Wicht, 'Characterization of mirror mount prototypes for RICH detectors', LHCb 2000-072 RICH

[6] E. Albrecht et al.; 'Perfluorocarbon effects on composite and polymeric materials used within RICH detectors', DELPHI 95-21 RICH 66

[7] M. Alemi, 'Passive magnetic shielding calculation for the photodetectors of RICH2', LHCb 98-017 RICH

M. Alemi, 'Tecniche di rivelazione nei RICH di LHCb', PhD thesis, Milano 1999

[8] T. Gys, 'The use of Pixel Hybrid Photon Detectors in the RICH counters of LHCb', LHCb 2000-064 RICH.

[9] S. Cuneo, M. Ameri, V. Gracco, P. Musico, A. Petrolini and M. Sannino, 'A proposal for a supporting structure for the Hybrid Pixel Detector of LHCb RICH 2', LHCb 2000-082 RICH

for a system with MaPMTs :

M. Ameri, S. Cuneo, P. Musico, A. Petrolini and M. Sannino, 'A proposal for a supporting structure for the multianode photomultipliers of RICH2', LHCb 2000-005 RICH

[10] C. D'Ambrosio, B. Franek, C. Gaspar, M. Laub, R. Lindner, F. Muheim, A. Papanestis and P. Soler, 'Monitoring, Alignment and control of the LHCb RICH detectors', LHCb 2000-080 RICH

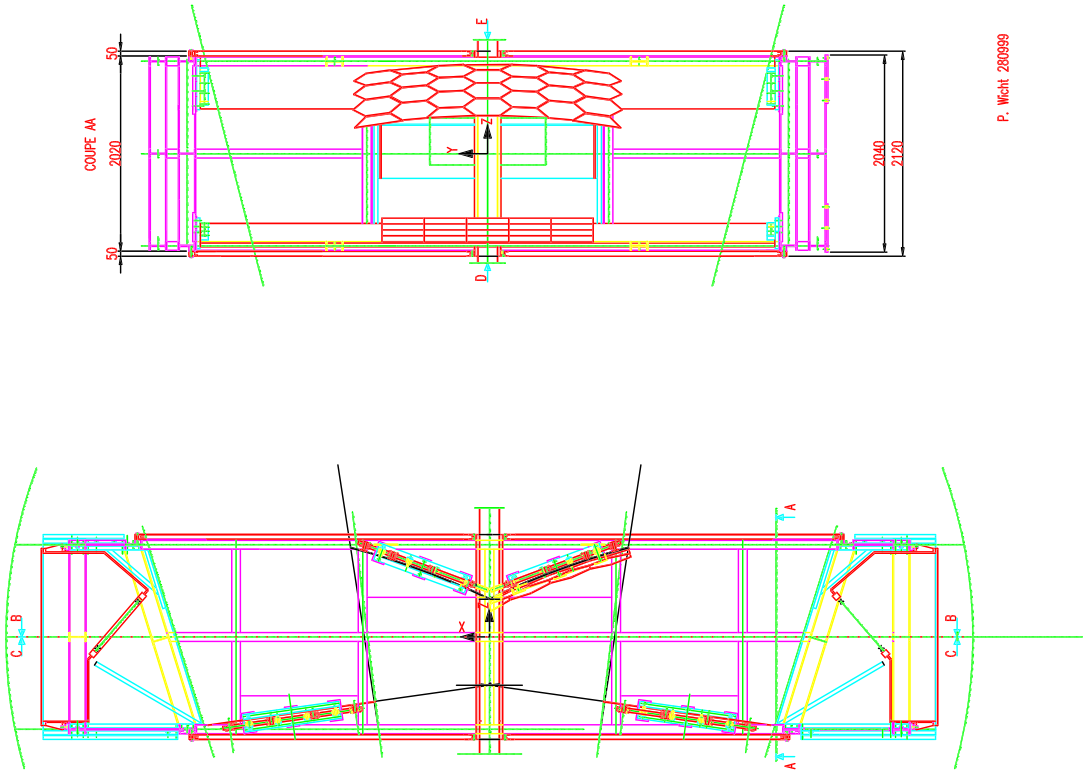

Figure 1: RICH 2 mechanics. Horizontal and side view.

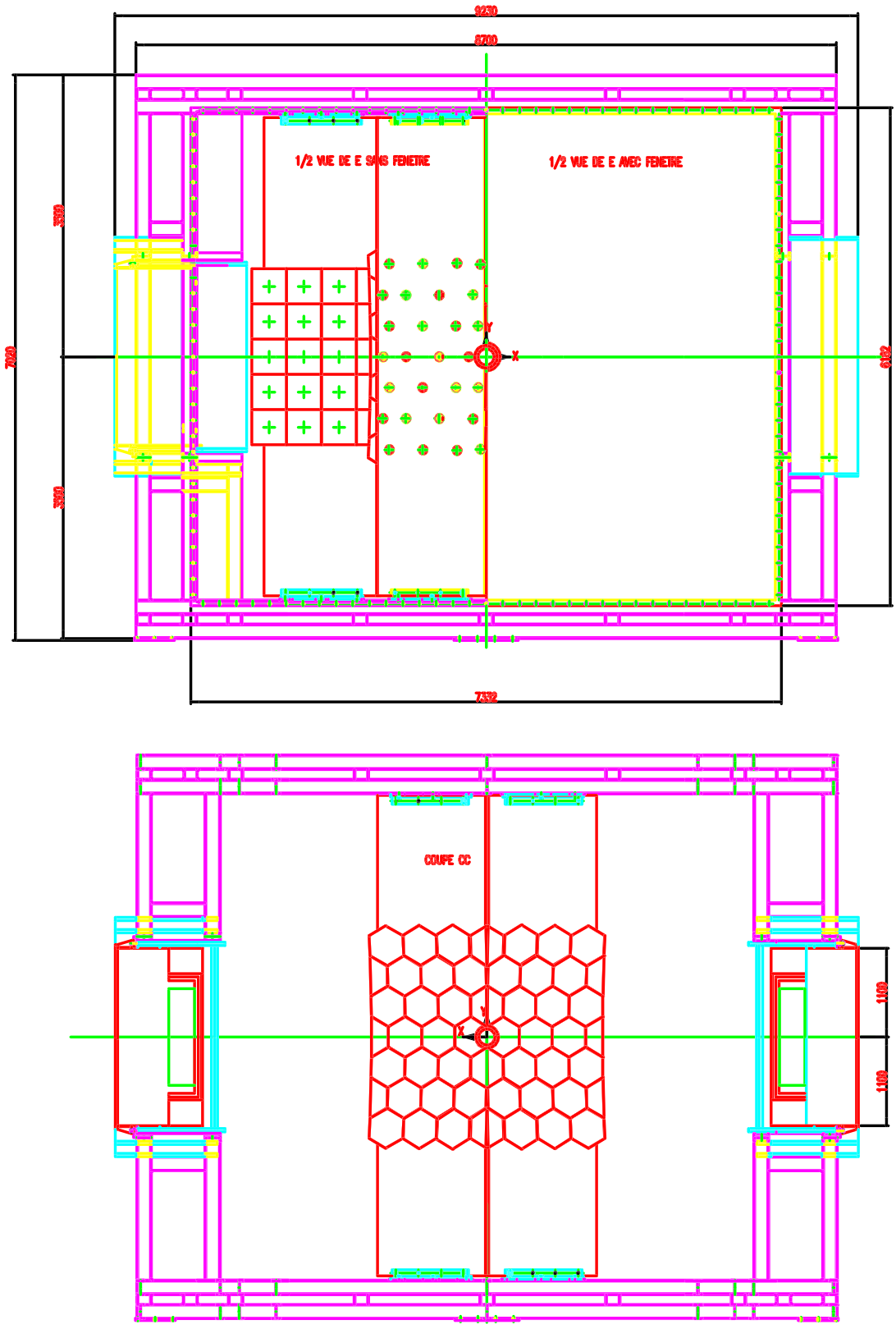

Figure 2: RICH 2 mechanics. Vertical projections.

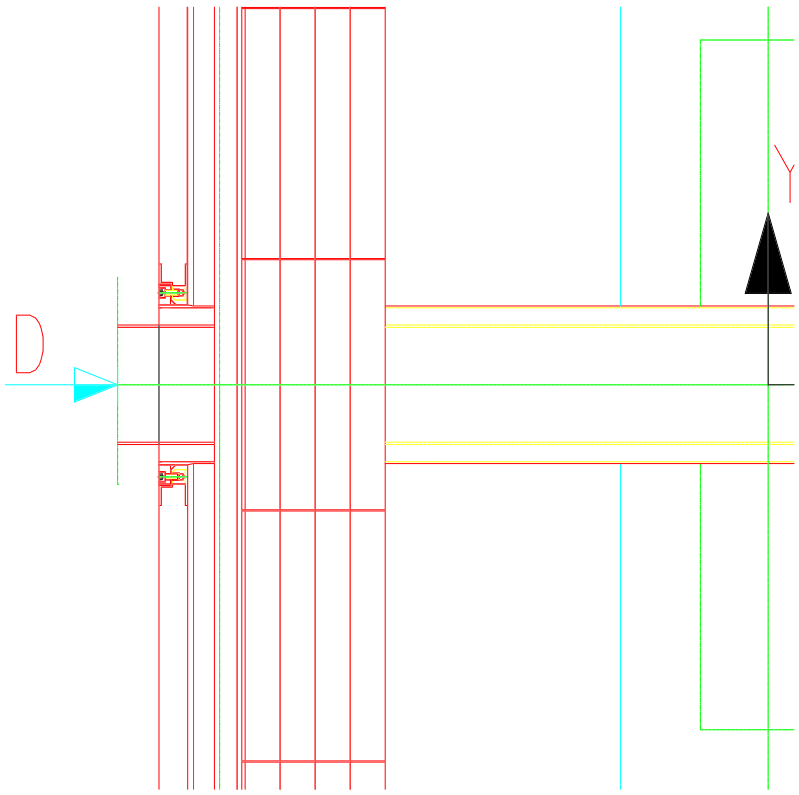

Figure 3: RICH 2 mechanics. Close-up of the central tube.

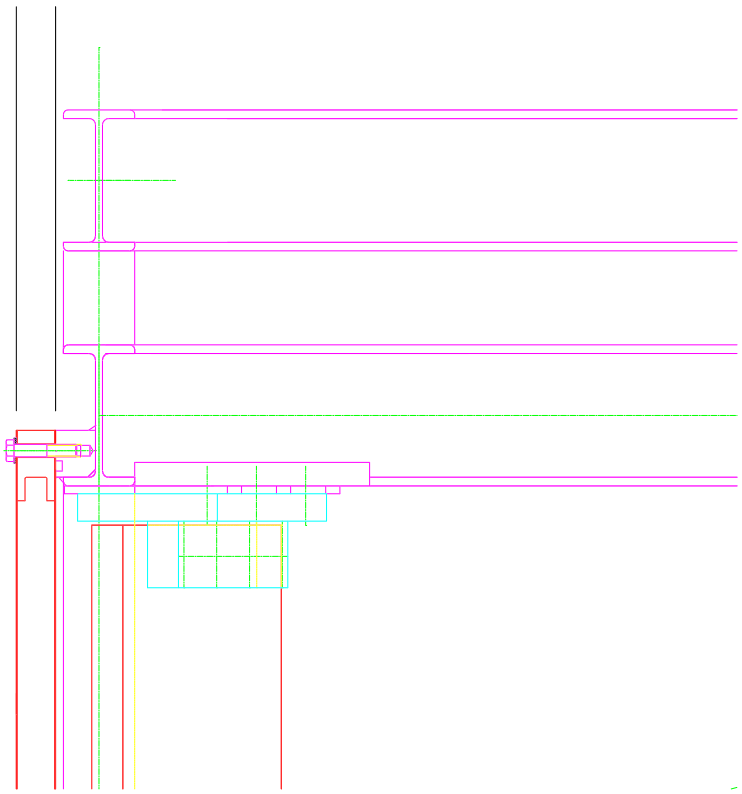

Figure 4: RICH 2 mechanics. Close-up of the junction between the window frame and the main structure.

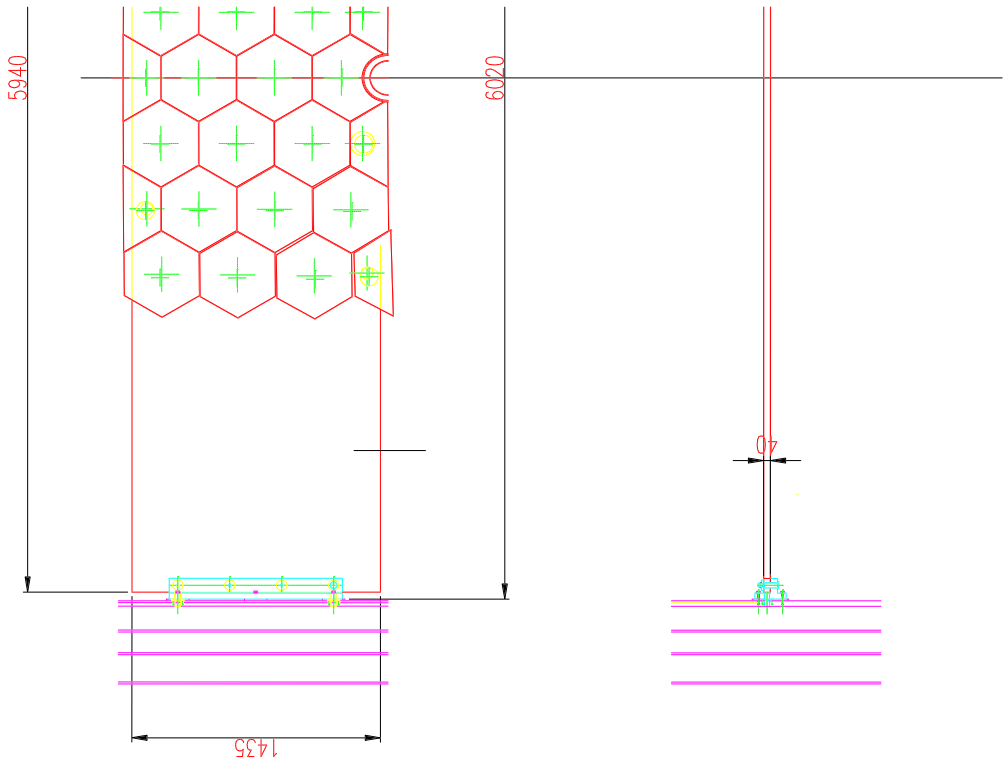

Figure 5: RICH 2 mechanics. Close-up of the mirror plate and the optical bench.

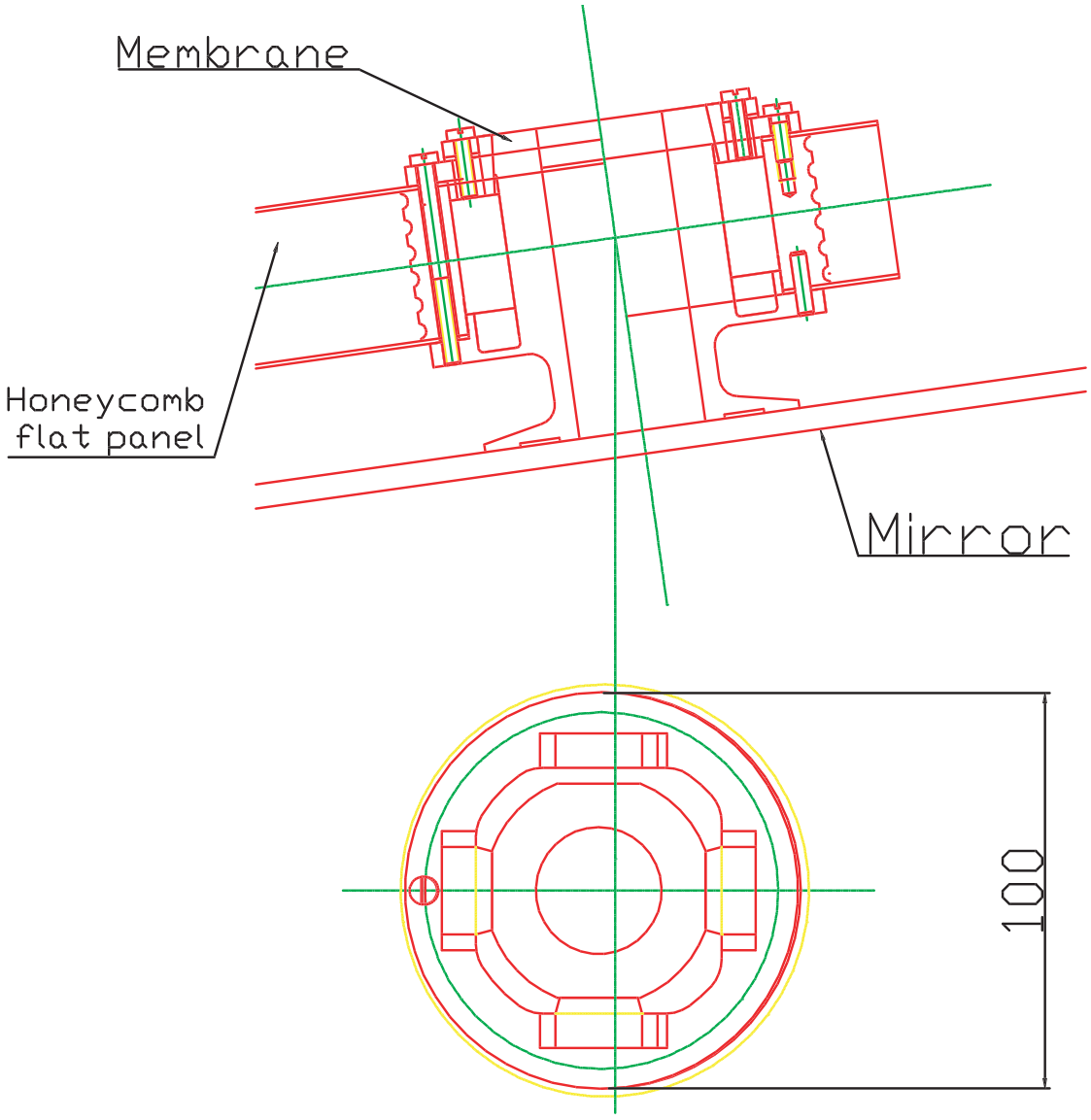

Figure 6: RICH 2 mechanics. The mirror support.

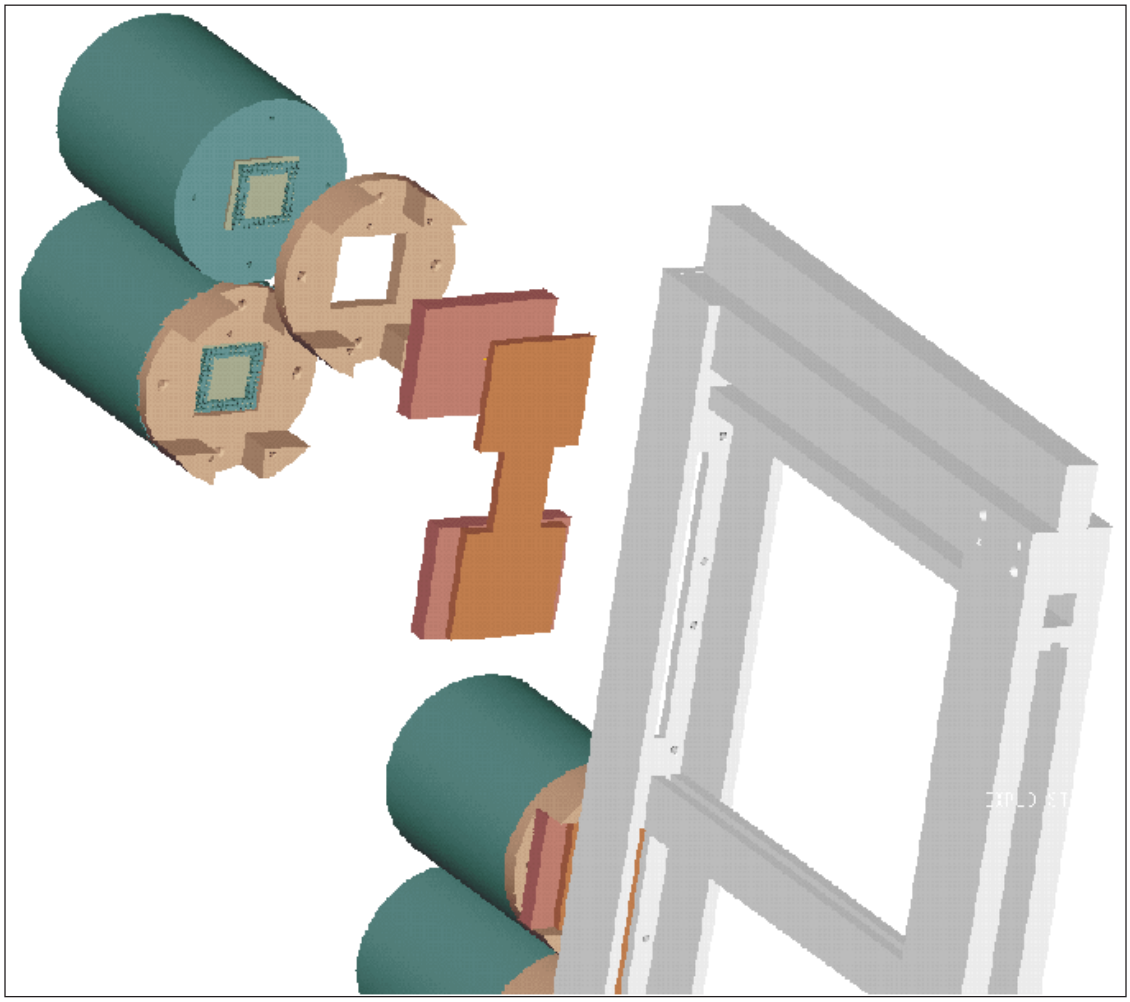

Figure 7: RICH 2 mechanics. The arrangement of the HPDs at the detector plane.

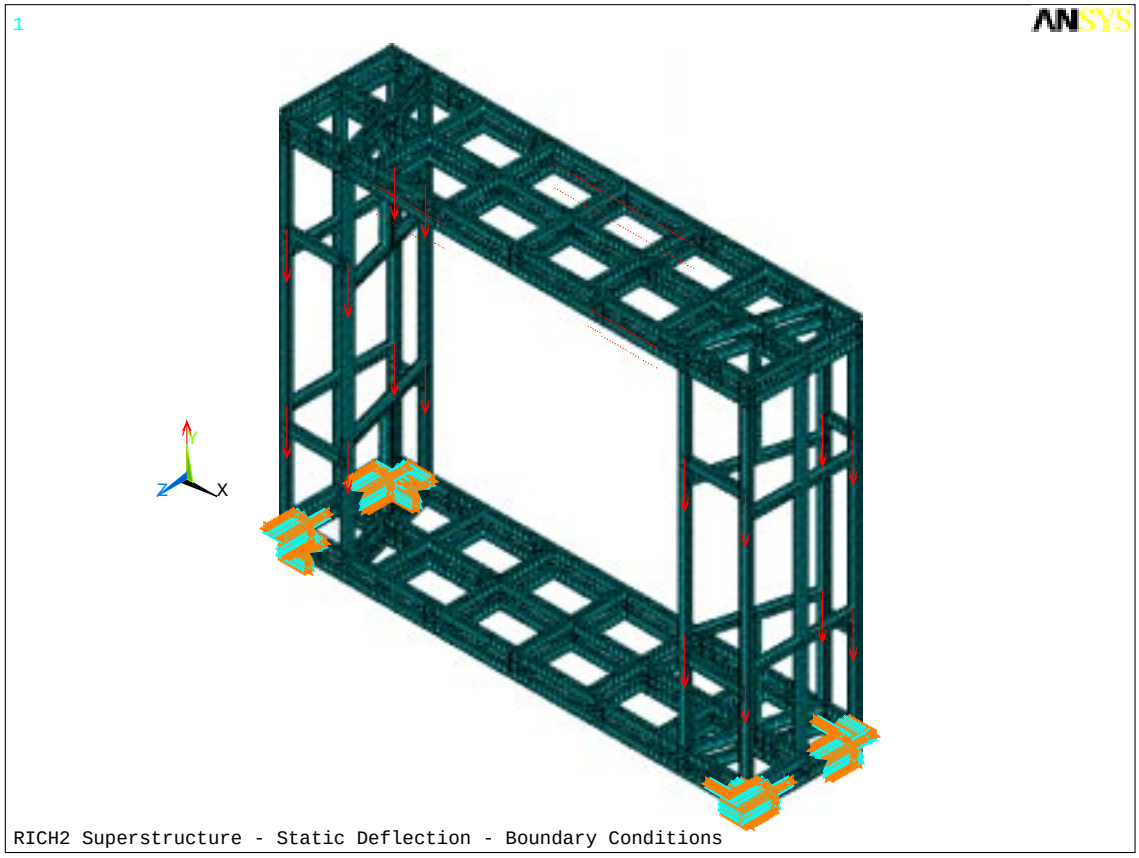

Figure 8: ANSYS analysis of RICH 2 structure. Initial conditions.

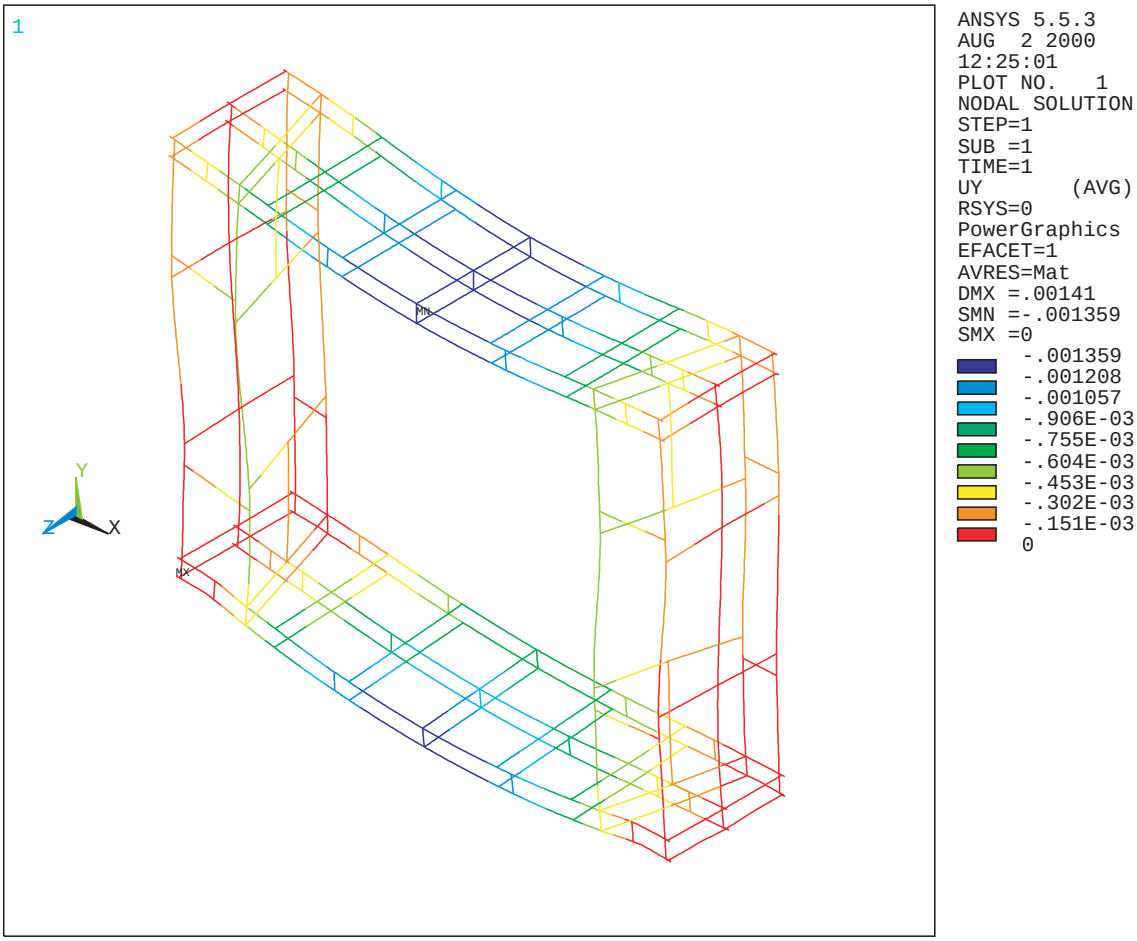

Figure 9: Static deflection of the RICH 2 space frame. Magnetic shielding and mirror plane included.

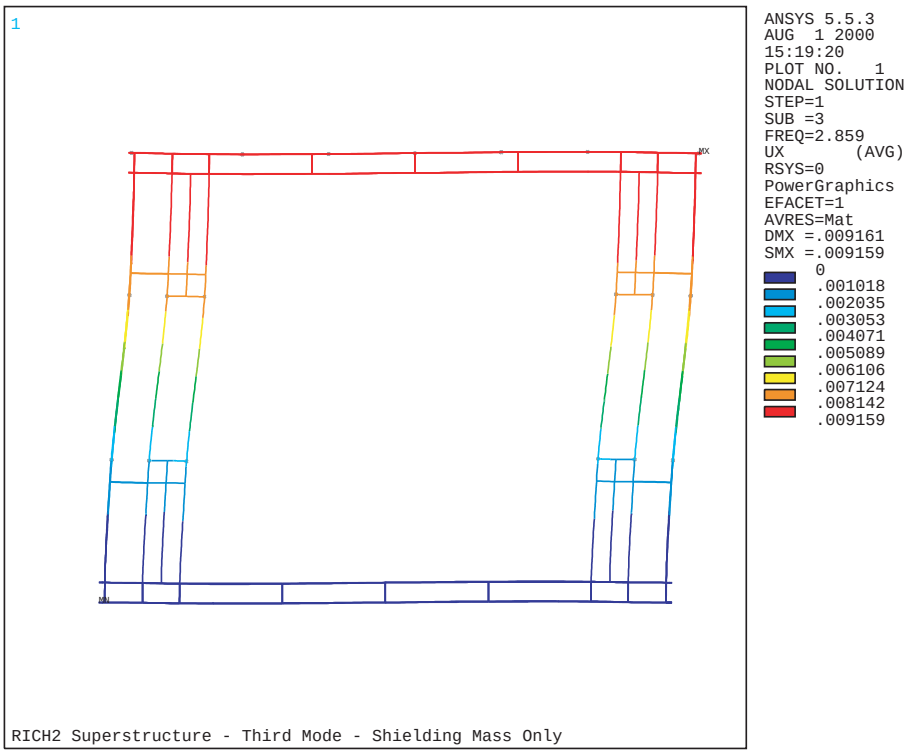

Figure 10: Mode 3 deflection of the RICH 2 space frame. Magnetic shielding and mirror plane included.

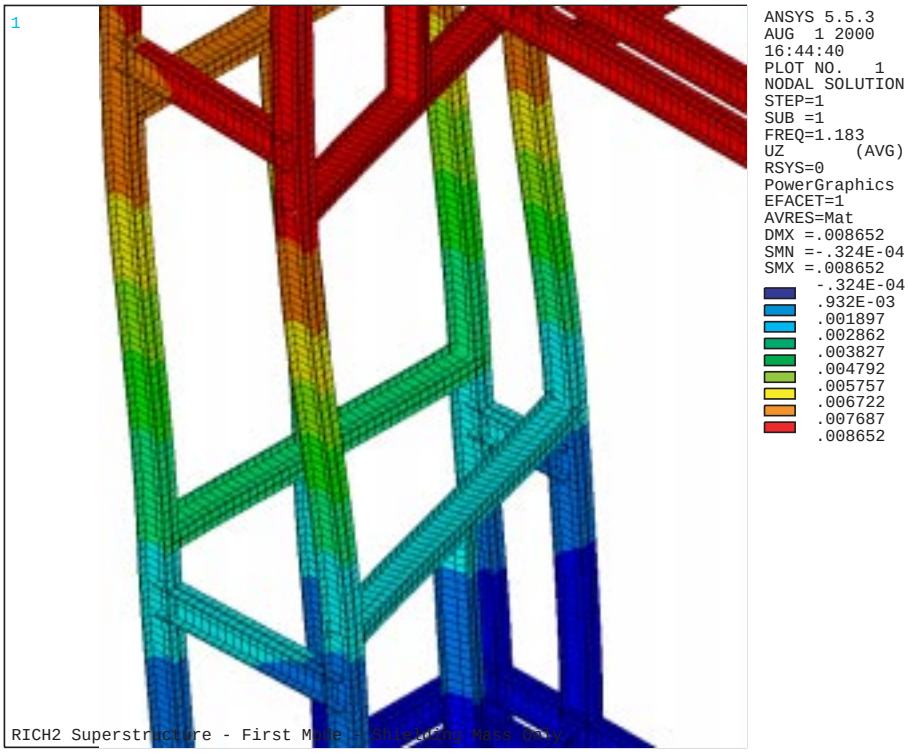

Figure 11: Mode 3 deflection of the RICH 2 space frame. Close-up for this mode next to the detector plane.